International Journal of Innovative Technology and Exploring Engineering (IJITEE)
ISSN: 2278-3075 (Online), Volume-4 Issue-7, December 2014

An Optimal Detection of Polyp and Ulcer in WCE Images using Fast BEMD with DLac Analysis"

Sharad T. Jadhav, Sanjay H. Dabhole

Abstract*— the main contribution of this paper is the presentation of a novel tool for WCE image analysis and classification by exploiting color-texture features. The proposed scheme has based on the ingenious combination of BEEMD and DLac, applied on the green/red component of WCE images in order to identify ulcerations. BEEMD, apart from an adaptive image denoising tool, was exploited to reveal the intrinsic components (IMFs) of the images in order to achieve data driven, Coefficient of Variance (CV), boost the distinctness between polyp and ulcer regions and facilitate DLac analysis to extract efficient texture characteristics. Optimum IMF selection based on the structure patterns of IMFs disclosed by DLac. The optimum IMFs are used to reconstruct a new refined image. The proposed approach has evaluated on selected WCE images, captured from patients, depicting ulcer and polyp tissue. The optimum image components (IMFs) that contain the majority of texture information include IMFs 5 and 8. Individual IMFs score up to 85.8% classification accuracy, while their exploitation as a group enhances the detection rate up to 94.3% for ulcer and polyp tissue.

***Keywords*— IMF, DLAC, CV, POLYP, Ulcer, WCE, EMD, BEEMD,GI,**

I. INTRODUCTION

A branch of medicine closely associated with one of these techniques, namely visual inspection, is gastro- enterology. In the field of gastroenterology, vision is widely understood as the fundamental mode of knowing the state of the gastrointestinal (GI) tract. The advent of medical imaging technologies, such as radiography (in the wider sense), tomography and especially endoscopy, promoted this paper by enabling the visual examination without demanding to gain physical access [4]. In case of visual inspection, as in case of auscultation, there are specific properties observed in order to assess the image content, no matter how simple or sophisticated the imaging technology is. During a stethoscope examination, for instance, the clinician attempts to identify frequency, pitch and duration deviations from the normal lung sounds. Similarly, during the observation of a medical image, there are image properties, corresponding to the acoustic ones of the pulmonary system, which may reveal the existence of illness. In the case of endoscopic GI tract images, these features essentially include texture, color and shape. The procedure that a clinician subconsciously follows in order to examine the images and reach a diagnosis is to seek for distortions. Distortions mainly in texture and color of the examined tissue, as compared to the features considered empirically or conceptually healthy.

Manuscript published on 30 December 2014.
***Correspondence Author(s)**
Sharad T. Jadhav, Ph.D Scholar, Department of Electronics and Communication, AISECT- Dr. C.V. Raman University, Kota, Bilaspur (C.G.), India.
Sanjay H. Dabhole, Ph.D Scholar, Department of Electronics and Communication, AISECT- Dr. C.V. Raman University, Kota, Bilaspur (C.G.), India.

While color and shape are quite tangible approaches, the concept of texture is more abstract and subjectively defined and interpreted; however, embodies valuable information that can be used to identify or describe an image [3]. The vagueness of this concept is evidenced by the fact that there is no universally agreed-upon definition of what image texture is and, in general, different researchers use different definitions depending upon the particular area of application [8]. The most widely used and accepted definition of texture in the field of medical image analysis, which is also adopted in this section, is the one that defines texture as the spatial variation of pixel intensities. In other words, texture describes the relationship between the intensities of neighboring pixels (not necessarily adjacent).

Texture is a fundamental characteristic that entails substantial information about the structural arrangement of surfaces and their relationship to the surrounding environment. This information may be applied to estimate shape, surface orientation, depth changes and construction materials. Texture is an innate property of virtually all surfaces; the grain of the wood, the weave of a fabric, the pattern of crops in a field, rugae on the mucous membrane of the stomach, the mucosa of colon and small intestine. An example of various texture patterns is given in Fig. 1. This structural information has been proven crucial for medical image analysis and [13]. This is the case especially for gastroenterology where the internal mucous membranes of the digestive tract exhibit strong textural features and distinctive patterns. For instance, an eroded ulcerous region or a protruded cancerous tissue is visually distinguished, mainly, by its alternated texture. Another image property also important for abnormal tissue evaluation is color. Ulcers, for instance, exhibit greenish-yellow hues while an active bleeding spot is characterized by deep red tones. On the contrary, the normal intestinal mucous membrane is reddish-pink in color. Nevertheless, color cannot be utilized as a standalone objective modality for abnormal tissue detection, since it is not perceptually uniform. The perceived color is highly conditioned by the nature and the amount of ambient luminosity [7]. Despite the color constancy effect [15] of the human color perception system, whereby the color perception of objects remains relatively constant under varying environmental and visual conditions, serious color variations and color casts exist because of the intervention of an endoscope or a camera between the intestinal tissue and the physician's eye [15]. For these reasons, gastroenterologists use color and texture information together, as the visual clues, along with other complementary examinations (i.e., blood tests, urine tests etc.), in order to reach a diagnosis.

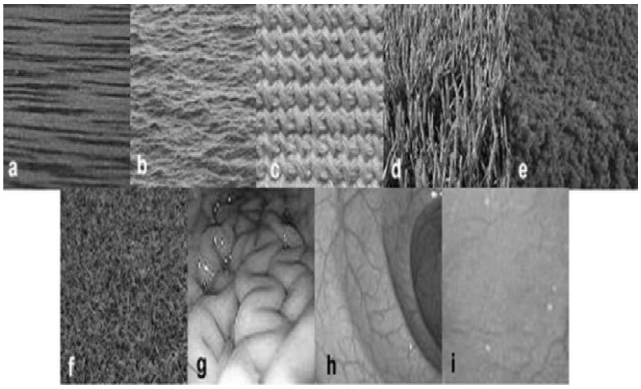

Figure 1. Digital images with visibly different texture regions: a) grain of wood, b) water, c)cloth, d) corn crops, e) forest, f) grass, g) stomach, h) colon, i) esophagus

The advent of Wireless Capsule Endoscopy (WCE) and the gastroenterologists' requirement for faster and more secure diagnoses necessitated the development of effective intestinal disorder recognition systems and automated WCE image analysis/inspection techniques.

II. WIRELESS CAPSULE ENDOSCOPY

In gastroenterology, the most common and established technique to visually inspect the GI tract and diagnose its diseases is endoscopy. The traditional endoscopic examinations applied for diagnosis in the upper and lower part of the GI tract, including esophagus, stomach, duodenum, terminal ileum and colon, are highly invasive causing discomfort to the patients. The visual inspection of the entire small intestine, in particular, has posed a challenge to gastroenterologists due to the strain of physically reaching it. Its important length and numerous windings make the examination extremely difficult, painful and not always possible, since usually there is a dead space in the middle part. Some imaging techniques used for the small intestine inspection include enteroclisis, small bowel follow through, push, sonde, and double balloon enteroscopy. Nevertheless, they are deeply inconvenient for the patients and require highly experienced gastroenterologists.

In 2000, advances in high integration and miniaturization allowed the researchers of Given Imaging to draw the attention of the GI community by unveiling what is now called endoscopic capsule. Wireless capsule endoscopy (WCE) is a novel medical procedure, which has revolutionized endoscopy, as it has enabled, for the first time, a painless and effective diagnosis inside the GI tract. A WCE system consists of the capsule endoscope, a data recorder system and computer software for WCE data processing. The capsule endoscope is a disposable, pill-shaped device which consists of a CMOS camera, four light sources, two batteries and a radio transmitter. The patient shallows the capsule which captures images of the GI tract at a speed of two frames per second (fps). These images are compressed with JPEG algorithm and transmitted wirelessly to a special recorder attached to the patient's waist. The entire process lasts approximately 8 hours until the batteries exhaust. Finally, the images stored in the recorder are downloaded to a computer and the physicians, with the aid of the special software, can review the images and analyze potential sources of various GI diseases. The capsule travels along the digestive tract with the physiological peristalsis, without the need for air in-sufflation and sedation. Thus, the examination of the entire small intestine has become the most comfortable endoscopic examination for the patient to undergo. In this way WCE is suitable even for children and elderly. WCE has proven invaluable in evaluating various diseases of the small bowel such as obscure bleeding, polyps and neoplasm, Crohn's disease, celiac disease and mucosal ulcers [1][24][29]. Ulcer is one of the most common lesions of the GI tract that affects approximately 10% of the people. The most usual causes are Helicobacter pylori bacteria and use of nonsteroidal antinflammatory drugs (NSAID). Ulcer is a chronic inflammatory sore or erosion on the internal mucous membranes that arises in small intestine, especially in duodenum (the upper part of the small intestine) and in stomach. Some serious diseases are associated with ulcer, like Crohn's disease and ulcerative colitis. Although ulcer by itself is not lethal, complications are capable of causing death. That is the reason why early diagnosis and treatment is extremely essential.

III. THE CONCEPT OF IMAGE DECOMPOSITION

Automated knowledge extraction from medical images is a last growing field of interest for the researchers. The attainment of this objective requires image decomposition to its components that will disclose the inherent structural characteristics of the image. In this context, this section presents Bidimensional Ensemble Empirical Mode Decomposition, a novel tool for image analysis.

3.1 Empirical Mode Decomposition (EMD)

In 1998, Huang *et al.* introduced a novel, intuitive and alternative signal decomposition technique for time-frequency analysis, namely Empirical Mode Decomposition (EMD) [28]. The major characteristic of EMD that renders it superior to traditional analysis methods, such as Fourier and Wavelets, is its adaptive nature. The decomposition does not require the use of *a priori* basis function. On the contrary, it is totally data driven. The concept that lies behind EMD is the existence of oscillations in every signal, at a very local level. Therefore, its target is to seek and reveal these inherent oscillatory modes, called Intrinsic Mode Functions (IMFs). EMD is designed to estimate IMFs of a signal so that, no matter how complicated the signal is, it embeds. A given signal x (t) can be decomposed into *n*

IMFs as:

$$x(t) = \sum_{n=1}^{n}(c_i + r_n) \quad (1)$$

Where c_i (t) is i^{th} IMF (IMF i) and r_n (t) is the low frequency trend of x (t) (residue). The highest frequency component of x (t) corresponds to the lowest value of index i, i.e., c_1 (t) (IMF1) While the value of *i* increases, lower frequency components are obtained.

Published By:
Blue Eyes Intelligence Engineering and Sciences Publication (BEIESP)

An example is given in Fig. 5a, where the signal is decomposed into five IMFs plus residue. The process to calculate each $c_i(t)$ is called sifting process. The local extrema are defined and interpolated, resulting in two fitting curves, one for the maxima and one for the minima. Then, the mean curve is calculated and subtracted from the signal. This procedure continues until a stopping criterion is satisfied. The signal that remains after the last subtraction is $c_1(t)$. Next, $c_1(t)$ is subtracted from the initial signal and the remainder constitutes the new initial signal on which the above procedure is applied in order to extract the following IMFs until the desired number is obtained.

3.2 Ensemble EMD (EEMD)

Despite the great advantage of EMD, deficiency arises when the extrema of the original signal are unevenly distributed. In such a case, the IMFs are incorrectly calculated, since either a single IMF contains signals of widely disparate scales or a single mode of oscillations resides in two or more IMFs. This phenomenon is called *mode mixing* and an example is depicted in Fig. 2b. It is clear that the first two IMFs, apart from the high frequency component of the signal, incorrectly include a low frequency oscillation. To overcome this issue, Huang *et al.* proposed a noise-assisted version of EMD, namely ensemble EMD (EEMD) [32]. EEMD requires the generation of an ensemble that contains multiple copies of the original signal that are distorted by white Gaussian noise, different for each copy, of finite amplitude. EMD is applied on every member of the ensemble and the final IMFs of the initial signal are derived by averaging the corresponding IMFs of each member of the ensemble. The concept of EEMD is grounded on the intuitive characteristics of white noise. White noise populates the whole time-frequency space uniformly and, as a result, establishes proper reference scales for the IMFs. The inherent modes of the signal are triggered by the noise and are projected accurately on the correct scales.

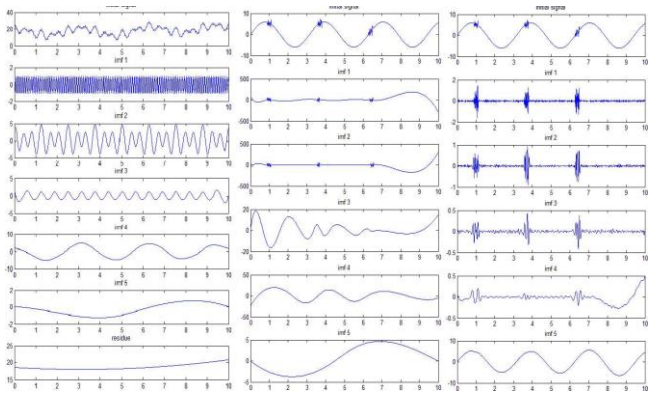

Figure 2. (a) EMD analysis, (b) mode mixing phenomenon, (c) ensemble EMD analysis

The IMFs of each ensemble member are noisy but the final average IMFs are noise free, since white noise cancels itself for a large number of ensemble members. Figure 2c presents the correct decomposition (using EEMD) of the signal in Fig. 2b. IMFs 1-3 include only the high frequency components while IMF5 contains the sinusoidal oscillation of the initial signal.

3.3 Bidimensional EEMD (BEEMD)

A multidimensional approach of EMD is required in case of a multidimensional signal. The extension of EMD in two dimensions (2D), namely Bidimensional EMD (BEMD), is an alternative multi-resolution analysis technique for image analysis and pattern discrimination. BEMD decomposes a 2D signal in 2D IMFs in the same way as eq. (1) demonstrates. However, there are two approaches for the realization of 2D extension. The first approach treats 2D data (images) as a collection of 1D slices (rows/columns) and applies 1D EMD on each row/column of the image (pseudo-BEMD). The second approach directly transplants the idea of 1D EMD algorithm in 2D data (genuine BEMD) after applying the appropriate changes (for example, fitting surfaces replace fitting curves). The first approach has the advantage of higher speed, while the latter exhibits improved performance, since the correlation among rows/columns of the image is taken into account. Bidimensional EEMD is the extension of EEMD in 2D [32].

IV. TEXTURE EXTRACTION

Texture is a major property of any image that is useful in machine vision applications, especially for medical purpose. There are many approaches for texture analysis proposed in the literature. This paragraph describes the concept of Differential Lacunarity, an efficient tool for texture features extraction and identification.

4.1 Lacunarity Analysis (Lac)

Lacunarity (Lac) was introduced by Mandelbrot as a fractal property, counterpart to fractal dimension that describes the texture of a fractal. Fractal dimension is a measure of how much space is filled without consideration about the space-filling characteristics of data [8]. In other words, two datasets with identical fractal dimensions can have distinct patterns with great differences in appearance. The introduction of Lac addressed this issue. Lac analyzes how space is filled and consequently, can discriminate textures and natural surfaces that share the same fractal dimension. In this direction, Lac has been used as a general technique to analyze patterns of spatial dispersion [28].The term "lacunarity" has been used to evaluate and describe the distribution of gap sizes along datasets. A set with gaps of widely disparate sizes is considered heterogeneous and is characterized by high Lac, while a homogeneous set, with uniform gap sizes, exhibits lower Lac. It should be highlighted that homogeneous sets at large scales can be quite heterogeneous when examined at smaller scales and vice versa. From this perspective, Lac can be considered as a scale dependent tool to measure the heterogeneity or texture of an object [2]. Various algorithms have been proposed to calculate and quantify Lac, but the most popular are based on the "gliding box algorithm" (GBA) straightforward and computationally simple. GBA is applicable on binary datasets, although it can be extended to real datasets by converting the numerical data to dyadic by thresholding [29] [32].

Published By:
Blue Eyes Intelligence Engineering
and Sciences Publication (BEIESP)

4.2 Differential Lacunarity Analysis (DLac)

Most real life, image analysis applications need to extract texture information from either grayscale or color images without the option of thresholding. To this end, Dong [2] introduced a new version of Lac, namely Differential Lacunarity (DLac), suitable for grayscale image analysis. DLac is calculated by a differential box counting method. This algorithm employs a gliding box *r* of size *r* x *r* pixels and a gliding window *w* of size *w* x *w* pixels with r<w.

Window *w* is initially positioned at the up left corner of the image and, by moving one by one columns to the left, scans the whole image. For every position of the window w, box r is placed inside the window at the up left corner and scans the image pixels bounded by the window (Fig. 3a) in order to calculate a value called "box mass". In other words, window *w* designates a region of the image (different each time until the entire image is covered) on which box mass is calculated with the aid of box *r*. According to the pixel values included in the box *(r* x *r* neighborhood) a column of more than one cubes of size (r x *r* x r) may be needed to cover the image intensity surface (Fig 3b). Numbers 1, 2, ... are assigned to the cubes from bottom to top and the differential height of the column *n(i,j)* is calculated (i, *j* is the position of the box). Let the minimum and maximum pixel values reside in the cubes u and v, respectively. The differential height of the column is defined as

$$n(i,j) = v - u - 1. \quad (2)$$

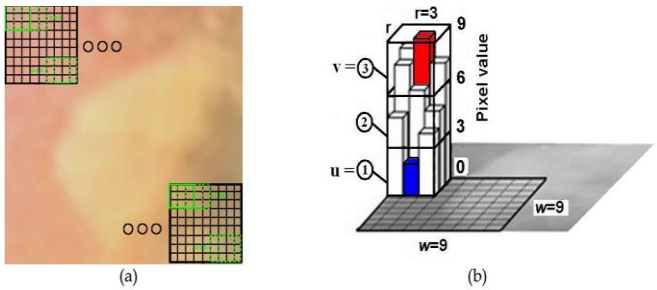

Figure 3. (a) gliding box (green) and gliding window (black) movement throughout the image,(b) differential box counting method for box mass calculation (box size r=3, window size w=9, differential height of the column n=3-1-1=1)

$$M = \sum_{n=i,j} n(i,j) \quad (3)$$

is the box mass of the window *w* at a specific place. Let (M,r) be the number of windows *w* with box mass M calculated by a box r. The probability function Q (M,r) is obtained by dividing n(M,r) by the total number of windows. The DLac of the image at scale *r* given a window *w* is defined as

$$\Lambda(r) = \frac{\sum_M M^2 Q(M,r)}{[\sum_M MQ(M,r)]^2} \quad (4)$$

V. THE PROPOSED AUTOMATED ULCER TISSUE IDENTIFICATION SCHEME

This section presents our proposed approach for color-texture-based automatic discrimination between ulcer and healthy tissue from WCE images. The color-texture concept was motivated by gastroenterologists' clinical practice, where the color and texture properties of WCE images are utilized for reaching a diagnosis. More specifically, our scheme, named CV-DLac, combines BEEMD analysis to achieve adaptive image refinement (CV) with DLac analysis for efficient extraction of ulcer texture information. BEEMD-Dlac combination for WCE image analysis was firstly introduced in [8]. The overall structure of the propose scheme is depicted in Fig.4.

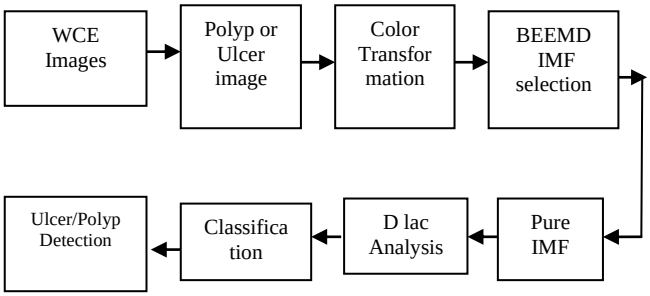

Figure. 4. The proposed BEEMD-DLac scheme

5.3.1 Proposed DLac analysis

The great advantage of DLac is the ability to perform texture analysis in various scales. The coarseness of the scale is primarily determined by the size of window w, which designates the size of the neighborhood for box mass calculation; the greater the window, the coarser the analysis scale. In the case of ulcer tissue recognition, a multi-scale texture analysis is required considering the great variability in size and appearance of ulcer regions. In this context, Dlac is calculated for a variety of window sizes, given a constant, relative small box size r, in order to achieve pattern analysis at different scales, while identifying slight variations in neighboring pixels (due to small value of r). An example of DLac-w (r=3, w=4-30) curves that correspond to images b, d, e and f from Fig. 1 is given in Fig. 5a.

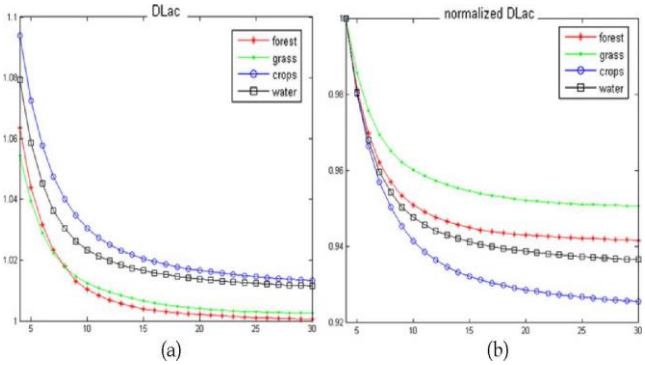

Figure 5. DLac (a) and normalized DLac (b) curves for various window sizes (4 to 30 pixels) for images b, d, e and f from Fig. 1

Published By:
Blue Eyes Intelligence Engineering
and Sciences Publication (BEIESP)

The curves are distinct; however, obvious discrimination is not achieved. To deliver greater differentiation between the curves an identical reference level has to be secured [28]. Thus, DLac-w curves are normalized to the DLac value that corresponds to the smallest *w*. The resulting curves (Fig. 5b) provide quite clear discrimination between the four patterns. From now on, any reference to DLac-w curves implies normalized curves. Optimized IMF selection is based on the characteristics of DLac-w curve of each IMF. The motive for such an approach lies in the concept that IMFs with possible useful texture information should provide DLac-w curves that bear resemblance to the curves estimated on ulcer images. In this context, it has been observed that the slope of DLac-w curves of ulcer images lies within specific limits for the majority of ulcer cases. This observation led us to a slope-based criterion for IMF selection. The IMFs that provide DLac curves with slopes within the limits, specified by DLac curves of ulcer images, were selected. Figure 6 shows the selection probability of each IMF. According to the diagram, IMF5, IMF6 and IMF8 were selected for the majority of images implying that the information included in these IMFs should be taken under consideration.

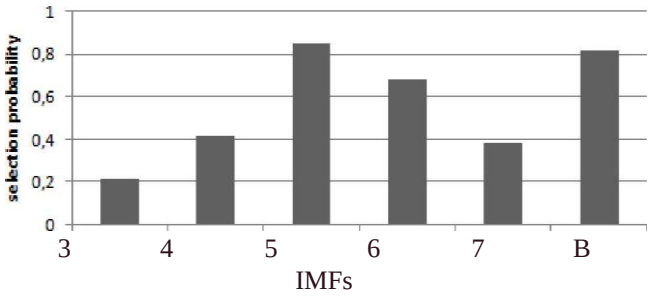

Figure 6. Selection probability for each IMF

VI. EXPERIMENTAL PHASE

The WCE images used in this study for the development and assessment of the proposed approach were drawn from six patients with ulcerous diseases, such as unexplained ulceration, ulceration from NSAID, ulcerative colitis and Crohn's diseases, who have undertaken a WCE examination in NIMTS Gastroenterology Clinic in Athens, Greece. The examinations were conducted with Pillcam SB (Given Imaging) WCE system. Rapid Reader 6.0 software (Given Imaging) was employed to export the images from the video sequence. The dataset collected consists of 87 ulcer and 87 polyp images. An example of the categories is given in Fig. 7. It must be highlighted that the 87 ulcer images were obtained from 87 different events (ulcer regions) to achieve the lowest possible similarity. Furthermore, the polyp images include both simple and confusing healthy tissue (folds, villus, bubbles etc.) The variety in image sizes does not affect the tissue discrimination procedure, since the feature vectors extracted from the images are utilized as the basis for comparison instead of the images themselves.

VII. RESULTS AND DISCUSSION

The performance of the proposed CV-DLac scheme is evaluated through the experimental results derived from the application of the introduced approach to the dataset described in fig. 7. To this end, results from every individual IMF analysis as well as results from both CV-DLac implementation scenarios are presented in this section.

7.1 Individual IMFs

Table 1 tabulates the classification performance achieved by the texture information extracted from each individual IMF for SVM classifier. The highest classification rates obtained for each IMF are noted in bold. The low classification rates for IMFs 1-2 denote their inefficiency in discriminating between ulcer and polyp tissue. The performance of IMF1, in terms of classification accuracy, becomes 62.9%, while the one of IMF2 is 63.5%. The sensitivity index is even lower (up to 44.9%) for the SVM classifier. This performance implies that the texture information that lies in IMFs 1 and 2 is not eligible for ulcer detection. This behavior is consistent with the concept of noise "contamination" of IMF1-2.

M_B	0.0025	0.0032	0.0038	0.0036
0.0030	0.34916	0.48959	0.61626	0.3018
CV	1.4412	8.4037	1.494	0.504
0.40088	0.00079	-0.00025	0.0012	0.0019
FD_{lac}				
1.4002				
C_{SVM} -				
0.0016				

Figure 7- a:Analysis of polyp sample images with specific coefficients

M_B	0.0031	0.0030	0.0034	0.0032
0.0024	0.2991	0.6685	0.5786	0.5241
CV	1.3918	9.2304	5.8205	3.4977
0.8762	-	-0.0015	-	-0.00071
FD_{lac}	0.00057		0.00021	
5.8490				
C_{SVM} -				
0.00019				

Figure 7-b: Analysis of ulcer sample images with specific coefficients

On the contrary, the classification accuracy of IMF3-8 is 78.5% to 84.55% improved. IMF3 and IMF4 exhibit the lowest (78.5%) and highest (80.8%) performance (in terms of accuracy), respectively. Despite the superior classification rates, the performance of individual IMFs indicates that texture information that resides in a single image component is inadequate for efficient ulcer detection.

Published By:
Blue Eyes Intelligence Engineering and Sciences Publication (BEIESP)

It should be highlighted that IMFs 5, 6 and 8, that are the most commonly selected IMFs in table 1, deliver the three highest classification accuracy rates among the IMFs. The convergence of these results testifies the optimal IMF selection procedure.

Table1. Mean classification accuracy, sensitivity and specificity (%) for each individual IMF (FVi, i=1 to 8), for SVM classifiers

IMF	SVM Classifier		
	Acc.	Sens.	Spec.
1	62.9	44.9	82.0
2	63.5	61.6	66.8
3	78.5	75.4	82.1
4	80.8	77.2	84.2
5	80.2	75.3	85.8
6	**83.6**	65.7	**82.2**
7	**83.8**	63.7	**84.8**
8	**84.55**	68.3	**94.3**

As far as the classification algorithms are concerned, the results in Table 1 and fig. 7 imply that the most efficient proposed system include coefficients of Dlac, coefficient of variance followed by classifier SVM. SVM achieves the best performance for the majority of IMFs (6-8) due to its more advanced nature for polyp and ulcer Images.

VIII. Overall Perspective and Future Work

The aforementioned experimental results highlight the potential of the proposed scheme towards ulcer and healthy intestinal tissue discrimination. The optimum image components (IMFs) that contain the majority of texture information include IMFs 5, 6 and 8. Individual IMFs score up to 84% classification accuracy, while their exploitation as a group enhances the detection rate up to 94.3%. When compared with other approaches, the proposed scheme seems to be more effective exhibiting increased classification ability by using a smaller feature vector. One of the most efficient ulcer detection approaches [8] used as a comparison baseline, and results in 82.6% accuracy when applied to our dataset [8]. In spite of the promising performance of the proposed scheme, there are still some issues for improvements that should be taken under consideration for its use in a future computer aided diagnosis system. Firstly, the number of ulcer and polyp images should be increased in order to secure maximum diversity between the ulcer cases develop more robust algorithms and obtain more accurate conclusions. Secondly, the computational cost of the proposed techniques should be revised. In this work, the introduction of a real time application was not our objective. In this context, the computational cost of the current unoptimized MATLAB code is 9.3 seconds per image, considering an average size of 256x256 pixels. BEEMD analysis consumes 83.4% of this time while DLac analysis and classification absorb 16.2% and 0.4%, respectively. When focusing on real time application, dedicated hardware and programming languages, more efficient implementation algorithms (for BEEMD and DLac) and multithreading programming should be considered.

IX. Conclusion

The proposed CV- DLac scheme is based on the ingenious combination of BEEMD and DLac, applied on the green component of ulcer and red component of Polyp WCE images in order to identify ulcerations. CV entailed optimum IMF selection is based on the structure patterns of IMFs disclosed by Dlac which is classified using SVM. Experimental results have shown that CV-DLac scheme exhibits quite outperform 3.42 % than existing method in [33]. Overall classification performance of intestinal texture information is distributed along IMFs 3 to 8. The classification performance of individual IMFs does not exceed 84.44% (classification accuracy), with IMF 8 being the most efficient.

However, the best results are delivered in the reconstruction case, where accuracy, sensitivity and specificity exceed 94.3%. The advanced overall classification performance of CV-Dlac followed by SVM approach paves the way for its use in a fully automatic diagnosis system.

References

1. Adler, S.N. & Metzger, Y.C. (2011). PillCam COLON capsule endoscopy: recent advances and new insights, *Therapeutic Advances in Gastroenterology*, Vol.4, No.4, pp. 265-268
2. Allain, C. & Coitre, M. (1991). Characterizing the lacunarity of random and deterministic fractal sets, *Physical Review a*, Vol.44, No.6, pp. 3552-3558
3. Ameling, S.; Wirth, S.; Paulus, D.; Lacey, G. & Vilarino, F. (2009). Texture-based polyp detection in colonoscopy, *Proc. of Bildverarbeitung fur die Medizin 2009*, pp. 364-350,
4. Aronott, I.D.R. & Lo, S.K. (2004). The clinical utility of wireless capsule endoscopy, *Digestive Diseases and Sciences*, Vol.49, No.6, pp. 893-901Berlin, Germany, March 22-25, 2009
5. Barkin, J.S. & Friedman, S. (2002). Wireless capsule endoscopy requiring surgical intervention: the world's experience, *The American Journal of Gastroenterology*, Vol.97, No.9, pp. S298
6. Belvin, ML.; Voderholzer, WA. & Loch, S. (2003). Diagnosing small intestinal strictures: first experience with the M2A patency capsule, *Endoscopy*, Vol.35, Suppl. II, pp. A184
7. Berlin, B. & Kay, P. (1969). Basic Color Terms: Their Universality and Evolution, *University of* California Press, ISBN 1-57586-162-3, Berkeley, California
8. Bourbakis, N. (2005). Detecting abnormal patterns in WCE images, *Proc. of 5th IEEE Symposium on Bioinformatics and Bioengineering*, pp. 232-238, Minneapolis, U.S.A., October 19-21, 2005
9. Capri, F.; Galbiati, S. & Capri, A. (2007). Controlled navigation of endoscopic capsules: Concept and preliminary experimental investigations, *IEEE Trans. on Biomedical Engineering*, Vol.54, No.11, pp. 2028-2036
10. Capri, F.; Kastelein, N.; Talcott, M. & Pappone, C. (2011). Magnetically Controllable Gastrointestinal Steering of Video Capsules, *IEEE Trans. on Biomedical Engineering*, Vol.58, No.2, pp. 231-234
11. Carta, R.; Thone, J. & Puers, R., Wireless power and data transmission for robotic endoscopic capsules, *Proc. of 12th Mediterranean Conference on Medical and Biological Engineering and Computing*, pp. 232-235, Chalkidiki, Greece, May 27-30

Published By:
Blue Eyes Intelligence Engineering and Sciences Publication (BEIESP)

12. Cauendo, A.; Rodriquez- Teilez, M.; Hernandez- Duran, M. *et al.* (2003). Evaluation of M2A patency capsule in the gastrointestinal tract: one-capsule preliminary data from a multicentre prospective trial, *Endoscopy*, Vol.35, Suppl.II, pp. A182 [a]Charisis, V. *et al.* (2010).
13. Abnormal Pattern Detection in Wireless Capsule Endoscopy Images Using Nonlinear Analysis in RGB Color Space, *Proc. of 32nd International Conference of IEEE Engineering in Medicine and Biology Society*, pp. 3674-3677, Buenos Aires, Argentina, August 31- September 4
[b]Charisis, V. *et al.* (2010).
14. Ulcer Detection in Wireless Capsule Endoscopy Images Using Bidimensional Nonlinear Analysis, *Proc. of 12th Mediterranean Conference on Medical and Biological Engineering and Computing*, pp. 236-239, Chalkidiki, Greece, May 27-30
15. Charisis, V.; Hadjileontiadis, L.J.; Liatsos, C.N.; Mavrogiannis, C.C. & Sergiadis, G.D. (2011). Capsule Endoscopy Image Analysis Using Texture Information from Various Color Models, *Computer Methods and Programs in Biomedicine*, under revision.
16. Cheifetz, A.S. *et al.* (2006). The risk of retention of the capsule endoscope in patients with known or suspected Crohn's disease, *The American Journal of Gastroenterology*, Vol.101, No.10, pp. 2218-2222
17. Coimbra, M. & Silva Cunha, J.P. (2006). MPEG-7 visual descriptors-contributions for automated feature extraction in capsule endoscopy, *IEEE Trans. on Circuits and Systems for Video Technology*, Vol.16, No.5, pp. 628-637
18. Cristianini, N. & Shawe-Taylor, J. (2000). *An Introduction to Support Vector Machines and Other Kernel-based Learning Methods*, Cambridge University Press, ISBN 0-52-178019-5, Cambridge, UK
19. Dong, P. (2000). Test of a new lacunarity estimation method for image texture analysis, *International Journal of Remote Sensing*, Vol.21, No.17, pp. 3369-3373
20. Fireman, Z. (2010). Capsule endoscopy: Future horizons, *World Journal of Gastrointestinal Endoscopy*, Vol.2, No.9, pp. 305-307
21. Foster, D.H. *et al.* (1997). Four issues concerning colour constancy and relational colour constancy, *Vision Research*, Vol.37, No.10, pp. 1341-1345
22. Foucault, M. (1973). *The Birth of the Clinic: An Archaeology of Medical Perception*, ISBN 0-415-30772-4, Pantheon Books, New York, USA
23. Friedman, S. (2004). Comparison of capsule endoscopy to other modalities in small bowl, *Gastrointestinal Endoscopy Clinics of North America*, Vol.14, No.1, pp. 51-60
24. Gao, M.; Hu, C.; Chen, Z.; Zhang, H. & Liu, S. (2010). Design and Fabrication of a Magnetic Propulsion System for Self-Propelled Capsule Endoscope, *IEEE Trans. on Biomedical Engineering*, Vol.57, No.12, pp. 2891-2902
25. Gefen, Y.; Meir, Y.; Mandelbrot, B.B. & Aharony, A. (1983). Geometric implementation of hypercubic lattices with noninteger dimensionality by use of low lacunarity fractal lattices, *Physical Review Letters*, Vol.50, No.3, pp. 145-148
26. Hadjileontiadis, L.J. (2009). A texture-based classification of crackles and squawks using lacunarity, IEEE Trans. on Biomedical Engineering, Vol.56, No.3, pp. 718-732
27. Haralick, R.M.; Shanmugam, K. & Dinstein, I. (1973). Textural features for image classification, *IEEE Trans. on Systems, Man and Cybernetics*, Vol.3, No.6, pp. 610-621
28. Huang, N.E. *et al.* (1998). The empirical mode decomposition and the Hilbert spectrum for nonlinear and non-stationary time series analysis, *Proc. of Royal Society of London a*, Vol.454, No.1971, pp. 903-995
29. Iakovidis, D.K.; Maroulis, D.E. & Karkanis, S.A. (2006). An intelligent system for automatic detection of gastrointestinal adenomas in video endoscopy, *Computers in Biology and Medicine*, Vol.26, No.10, pp. 1084-1103
30. Iddan, G.; Meron, G.; Glukhovsky, A. & Swain, P. (2000). Wireless capsule endoscopy, *Nature*, Vol.405, No.6785, pp. 417-417
31. Julesz, B. (1975). Experiments in the visual perception of texture, *Scientific American*, Vol. 232, No.4, pp 34-43
32. Karkanis, S.A.; Iakovidis, D.K.; Maroulis, D.E.; Karras, D.A. & Tsivras, M. (2007). Computer- aided tumor detection in endoscopic video using color wavelet features, *IEEE Trans. on Information Technology in Biomedicine*, Vol.7, No.3, pp. 142-151
33. [a]Kodogiannis, V.S.; Boulougoura, M.; Lygouras, J.N. & Petrounias, I. (2007). A neuro-fuzzy- based system for detecting abnormal patterns in wireless-capsule endoscopic images, *Neurocomputing*, Vol. 70, No.4-6, pp. 704-717
34. Kodogiannis, V.S.; Boulougoura, M.; Wadge, E. & Lygouras, J.N. (2007). The usage of soft- computing methodologies in interpreting capsule endoscopy, *Engineering Applications of Artificial Intelligence*, Vol.20, No.4, pp. 539-553
35. Krzanowski, W.J. (2000). *Principles of multivariate analysis: A user's perspective*, Oxford University Press, ISBN 0-19-850708-9, New York, USA
36. Li, B. & Meng, M.Q.-H. (2007). Analysis of the gastrointestinal status from wireless capsule endoscopy images using local color feature, *Proc. of 2007 International Conference on Information Acquisition*, pp. 553-557,
37. [b]Li, B. & Meng, M. Q.-H. (2009). Texture analysis for ulcer detection in capsule endoscopy images, *Image and Vision Computing*, Vol.27, No.3, pp. 1336-1342
Liao, Z.; Gao, R.; Xu, C. & Li, ZS. (2010). Indications and detection, completion, and retention rates of small-bowel capsule endoscopy: a systematic review, *Gastrointestinal Endoscopy*, Vol.71, No.2, pp. 280-286

AUTHOR PROFILE

Prof. Sanjay H. Dabhole, last six years working as Principal in Sant Gajanan Maharaj Rural Polytechnic, Mahagaon, Gadhinglaj Tahsil, dist-Kolhapur. (M.S), INDIA, obtained his Bachelor's Degree of Electronics Engineering in 2002 from Walchand College of Engineering Sangli at Shivaji University, Kolhapur M.S., and took his Masters Degree of Electronics and Telecommunication Engineering in 2006 from KIT C.O.E. of Shivaji University Kolhapur with first rank, M.S. Currently, he is pursuing Ph.D from Electronics and Communication Dept. AISECT- Dr. C.V. Raman University, Kota. Bilaspur (C.G.), INDIA. I have total 12 years of teaching experience at various technical institutes and setup new Sant Gajanan Maharaj Technical campus in all aspects within 4 years. National level Best Teacher award on occasion of World teachers' day on 5th Oct. 2014 from Aviskar Social was Received and Educational Foundation Kolhapur (M.S.), INDIA. I am life time member of The Institution of Engineers, India. (IEI) apex body and his area of interest is Signal & Image Processing. To his credit 12 papers have been published in International & National Conferences and six papers have been published in International journals including IEEE explore whose impact factor is more than 1.0.

Prof. Sharad T. Jadhav, last three years working as an I/c Head and Asst. Professor in Dept. of Electronics and Telecommunication at Sanjeevan Engg. & Tech. Institute, Panhala. Dist-Kolhapur. (M.S), INDIA, obtained his Bachelor's Degree of Electronics Engineering in 2001 from Pune University, Pune M.S., and took his Masters Degree of Electronics and Telecommunication Engineering in 2007 from KIT C.O.E. of Shivaji University Kolhapur. (M.S.) Currently, he is pursuing Ph.D from Electronics and Communication Dept. AISECT- Dr. C.V. Raman University, Kota. Bilaspur (C.G.), INDIA. I have total 13 years of teaching experience at various technical institutes I am life time member of ISTE and IETE New Delhi apex body and his area of interest is Bio-medical & Image Processing. To his credit 10 papers have been published in International & National Conferences and one paper has been published in IJEA, Vol. 3, Special Issue 1, and ISSN: 2320 – 0804(o) International journal.

Published By:
Blue Eyes Intelligence Engineering and Sciences Publication (BEIESP)

Published By:
Blue Eyes Intelligence Engineering
and Sciences Publication (BEIESP)